Journal of Computational Physics 245 (2013) 281–301

Contents lists available at SciVerse ScienceDirect

Journal of Computational Physics

journal homepage: www.elsevier.com/locate/jcp

# A convergence study for SPDEs using combined Polynomial Chaos and Dynamically-Orthogonal schemes

Minseok Choi [a], Themistoklis P. Sapsis [b], George Em Karniadakis [a,*]

[a] Division of Applied Mathematics, Brown University, Providence, RI 02912, USA
[b] Courant Institute of Mathematical Sciences, New York University, NY 10012, USA

ARTICLE INFO

*Article history:*
Received 20 January 2012
Received in revised form 14 November 2012
Accepted 28 February 2013
Available online 25 March 2013

*Keywords:*
Stochastic partial differential equations
Uncertainty quantification
High dimensions
Stochastic collocation
Low-dimensionality

ABSTRACT

We study the convergence properties of the recently developed Dynamically Orthogonal (DO) field equations [1] in comparison with the Polynomial Chaos (PC) method. To this end, we consider a series of one-dimensional prototype SPDEs, whose solution can be expressed analytically, and which are associated with both linear (advection equation) and nonlinear (Burgers equation) problems with excitations that lead to unimodal and strongly bi-modal distributions. We also propose a hybrid approach to tackle the singular limit of the DO equations for the case of deterministic initial conditions. The results reveal that the DO method converges exponentially fast with respect to the number of modes (for the problems considered) giving same levels of computational accuracy comparable with the PC method but (in many cases) with substantially smaller computational cost compared to stochastic collocation, especially when the involved parametric space is high-dimensional.



## 1. Introduction

Recently, there has been a growing interest in quantifying parametric uncertainty in mathematical physics problems through the probabilistic framework. Such problems are often described by stochastic partial differential equations (SPDEs), and they arise in fluid mechanics, solid mechanics, wave propagation through random media [2–4], random vibrations [5–7], etc. The source of stochasticity in all the above cases includes uncertainty in physical parameters, initial and/or boundary conditions, random excitations, etc. All these stochastic elements may be modeled as random processes or random variables. Several methods have been developed to study SPDEs, including the Monte Carlo (MC) method and its variants and, more recently, Polynomial Chaos (PC) and its variants. One of the often neglected issue in developing new numerical methods is the study of the convergence properties of the method, which is especially important for stochastic solutions that lack regularity and they are typically high-dimensional.

The Polynomial Chaos (PC) method was developed in [8] in the context of the Wiener–Hermite polynomial chaos expansion. The stochastic processes are represented by a series of Hermite polynomials in terms of random variables. A Galerkin projection of the governing equations to the low-dimensional subspace spanned by Hermite polynomials yields a set of deterministic equations. PC has been applied to many problems including structural mechanics [9–11], fluid mechanics [12–16], etc. The generalized polynomial chaos developed by [14,17] employ non-Hermite polynomials to improve efficiency for a wider class of nonlinear problems. A computationally efficient version of PC is the probabilistic collocation method (PCM; also referred to as stochastic collocation), which exhibits fast convergence rates with increasing order of the

* Corresponding author. Tel.: +1 401 863 1217; fax: +1 401 863 2722.
*E-mail address:* george_karniadakis@brown.edu (G.E. Karniadakis).

0021-9991/$ - see front matter © 2013 Elsevier Inc. All rights reserved.
http://dx.doi.org/10.1016/j.jcp.2013.02.047

expansions, provided that solutions are sufficiently smooth in the parametric space [18–20]. In particular, the multi-element PCM (ME–PCM) is very effective for problems with parametric discontinuities [20].

A new approach, called Dynamically Orthogonal (DO) method, was developed in [1]; the idea is to represent the solution in a more general expansion, i.e.,

$$u(x,t;\omega) = \bar{u}(x,t) + \sum_{i=1}^{N} Y_i(t;\omega)u_i(x,t),$$

where $Y_i(t;\omega)$ are stochastic processes, $u_i(x,t)$ orthonormal fields and $\bar{u}(x,t)$ is the mean. The time dependence on *both* the stochastic coefficients and the basis fields makes the above representation very flexible for the representation of strongly transient, non-stationary responses. However, this same property makes the representation redundant and the derivation of well-posed equations for all the quantities involved is not a straightforward problem. In [1] it was illustrated how this redundancy can be overcome by adopting a natural constraint: *the dynamical orthogonality condition*. It was shown that using this condition a set of evolution equations for the $Y_i(t;\omega), u_i(x,t)$ and $\bar{u}(x,t)$ can be derived. These derived field equations are consistent with existing methods such as proper orthogonal decomposition method (POD) and PC.

From a computational point of view the evolution of uncertainty using the DO framework is performed by solving a set of $(N+1)$ deterministic PDEs together with $N$ (ordinary) stochastic differential equations (SDE). The system of PDEs describes the evolution of the mean field and the basis elements that define the stochastic subspace where uncertainty 'lives'. The SDE on the other hand defines how the stochasticity will be evolved within the reduced-order stochastic subspace. In the limit of very small uncertainty the DO equations reach a singular limit where the modes evolve independently from the statistics within the subspace. This limit may create important numerical problems since it involves the calculation of ratios of very small moment quantities. From a practical point of view the above situation can be very important especially in problems involving deterministic initial conditions. In such a case (deterministic initial state) another issue rises and this is the initialization of the stochastic subspace (since any initial choice of modes is allowable).

To tackle this issue we develop a hybrid method to overcome this singularity by combining the PC method with the DO method. Initially, the SPDEs are solved by the PC (e.g. via PCM or ME–PCM), and as the stochasticity develops we switch over to the DO method. This hybrid approach also gives us a set of modes, which are used to initiate the stochastic subspace. We consider three one-dimensional SPDEs which are associated with linear (advection equation) and nonlinear (Burgers and diffusion equation). For the advection equation the solution can be expressed analytically. For Burgers equation we consider two other cases: one has the analytical solution with excitation functions that lead to unimodal and bi-modal distributions while the other has random forcing. For the diffusion equation we consider the unsteady heat equation with uncertain inputs in heat conductivity that is multi-dimensional in parametric space. In particular, we examine the convergence of the new hybrid method and compare its accuracy and the efficiency with the PCM, which is the golden standard in uncertainty quantification at the present time.

The remaining part of the paper is organized as follows. In Section 2 we briefly review the DO representation and the corresponding evolution equations. Subsequently, we present the hybrid method of PC and DO. In the following sections, the hybrid method is applied to two SPDEs. In Section 3, a stochastic advection equation is considered; the exact formulas for the stochastic coefficients and deterministic basis are given and comparison with PCM is presented. In Section 4, two Burgers equations are considered. First, the Burgers solution is constructed given the stochastic coefficients and basis and the corresponding exact PDF is derived. Second, the Burgers equation is considered for testing the hybrid method and convergence with respect to the number of modes. In Section 5, the nonlinear diffusion equation is considered; it is multi-dimensional in parametric space with no exact solution and the convergence with respect to the number of modes is presented. We conclude the paper with a brief summary in Section 6.

## 2. An overview of the DO equations and a new hybrid DO-PC approach

We consider the following SPDE:

$$\frac{\partial u}{\partial t} = \mathscr{L}(u(t,x;\omega)), \quad x \in D, \quad \omega \in \Omega \tag{1a}$$

$$u(t_0,x;\omega) = u_0(x;\omega), \quad x \in D, \quad \omega \in \Omega \tag{1b}$$

$$\mathscr{B}[u(t,x;\omega)] = h(t,x;\omega), \quad x \in \partial D, \quad \omega \in \Omega, \tag{1c}$$

where $\mathscr{L}$ is a differential operator and $\mathscr{B}$ is a linear differential operator. $D$ is a bounded domain in $\mathscr{R}^d$ where $d = 1, 2$, or 3.

### 2.1. Definitions

Let $(\Omega, \mathscr{F}, P)$ be a probability space, where $\Omega$ is the sample space, $\mathscr{F}$ is the $\sigma$-algebra of subsets of $\Omega$, and $P$ is a probability measure. For a random field $u(x,t;\omega)$, $\omega \in \Omega$, the expectation operator of $u$ is defined as

$$\bar{u}(x,t) = E[u(x,t;\omega)] = \int_{\Omega} u(x,t;\omega)dP(\omega).$$

The set of all continuous and square integrable random fields, *i.e.*, $\int_D E[u(x,t;\omega)^T u(x,t;\omega)]dx < \infty$, where $u(x,t;\omega)^T$ is the transpose of $u$, for all $t \in T$ and the bi-linear form of the covariance operator

$$C_{u(\cdot,t;\omega)v(\cdot,s;\omega)}(x,y) = E[(u(x,t;\omega) - \bar{u}(x,t))'(v(x,s;\omega) - \bar{v}(x,s))], \quad x,y \in D,$$

form a Hilbert space that will be denoted by $\mathscr{H}$ [2,21]. For $u(x,t;\omega), v(x,t;\omega) \in \mathscr{H}$, the spatial inner product is defined as

$$\langle u(\cdot,t;\omega), v(\cdot,t;\omega)\rangle = \int_D u(x,t;\omega)^T v(x,t;\omega)dx.$$

We define the projection operator $\Phi_S$ of a field $u(x,t), x \in D$ to an $m$-dimensional linear subspace $S$ spanned by the orthogonal basis $S = \{w_i(x,t;\omega)\}_{i=1}^m, x \in D$ as follows:

$$\Phi_S[u(x,t;\omega)] = \sum_{i=1}^m \langle w_i(\cdot,t;\omega), u(\cdot,t;\omega)\rangle w_i(x,t;\omega)$$

### 2.2. DO representation

The DO equations are briefly described in the following subsections; see [1] for more details. Using a time-dependent generalization of the Karhunen–Loeve (KL) expansion [1], we have that every random field $u(x,t;\omega) \in \mathscr{H}$ at a given time $t$ can be approximated by a finite series of the form

$$u(x,t;\omega) = \bar{u}(x,t) + \sum_{i=1}^N Y_i(t;\omega)u_i(x,t), \tag{2}$$

where $u_i(x,t)$ are the eigenfunctions, and $Y_i(t;\omega)$ are zero-mean stochastic processes whose variance $E[Y^2(t;\omega)]$ is equal to the corresponding eigenvalue $\lambda_i(t)$ of the eigenvalue problem of the Karhunen–Loeve decomposition:

$$\int_D C_{u(\cdot,t)u(\cdot,t)}(x,y)u_i(x,t)dx = \lambda_i(t)u_i(y,t), \quad y \in D. \tag{3}$$

We define the linear subspace $V_S = span\{u_i(x,t)\}_{i=1}^N$ as the linear space spanned by the $N$ deterministic eigenfields associated with the $N$ largest eigenvalues. Note that both the stochastic coefficients $Y_i(t;\omega)$ and the orthogonal basis $u_i(x,t)$ are time-dependent (and they are evolving according to the system dynamics) unlike other methods such as the standard PC where the stochastic coefficients are time-independent. In [22], a similar expansion with time evolving PC basis is presented but the time-depended basis is obtained according to the PDF of the solution; in DO it is obtained through an evolution equation as we explain next.

### 2.3. DO field equations

All quantities $\bar{u}(x,t), u_i(x,t), Y_i(t;\omega),\ i = 1,\ldots,N$ in the representation (2) are time-dependent and hence there exists some redundancy in the representation. Therefore, additional constraints need to be imposed in order to formulate a well posed problem for the unknown quantities. As first proposed in [1], a natural constraint to overcome redundancy is that the evolution of the basis $\{u_i(x,t)\}_{i=1}^N$ be *normal* to the space $V_S$; this can be expressed through the following condition:

$$\frac{dV_S}{dt} \perp V_S \Longleftrightarrow \left\langle \frac{\partial u_i(x,t)}{\partial t}, u_j(x,t) \right\rangle = 0 \quad i,j = 1,\ldots,N. \tag{4}$$

This condition is referred to as the *dynamically orthogonal (DO) condition*. Note that the DO condition preserves orthonormality of the basis $\{u_i(x,t)\}_{i=1}^N$ since

$$\frac{\partial}{\partial t}\langle u_i(\cdot,t), u_j(\cdot,t)\rangle = \left\langle \frac{\partial u_i(\cdot,t)}{\partial t}, u_j(\cdot,t) \right\rangle + \left\langle u_i(\cdot,t), \frac{\partial u_j(\cdot,t)}{\partial t} \right\rangle = 0, \quad i,j = 1,\ldots,N.$$

It is proved in [1] that the DO condition leads to a set of independent and explicit evolution equations for all the unknown quantities. Next, we state the DO evolution equations without proof:

**Theorem 1.** *Under the assumptions of the DO representation, the original SPDE (1a,1b,1c) is reduced to the following system of equations*

$$\frac{\partial \bar{u}(t,x)}{\partial t} = E[\mathscr{L}[u(\cdot,t;\omega)]], \tag{5a}$$

$$\frac{dY_i(t;\omega)}{dt} = < \mathscr{L}[u(\cdot,t;\omega)] - E[\mathscr{L}[u(\cdot,t;\omega)]], u_i(\cdot,t) >, \quad i = 1,\ldots,N \tag{5b}$$

$$\sum_{i=1}^N C_{Y_i(t)Y_j(t)} \frac{\partial u_i(t,x)}{\partial t} = \prod_{V_S^\perp} E[\mathscr{L}[u(\cdot,t;\omega)]Y_j], \quad j = 1,\ldots,N, \tag{5c}$$

*where the projection in the orthogonal complement of the linear subspace is defined as* $\prod_{V_S^\perp} F(x) = F(x) - \prod_{V_S} F(x) = F(x) - \sum_{k=1}^{N} \langle F(\cdot), u_k(\cdot,t)\rangle u_k(\cdot,t)$ *and the covariance of the stochastic coefficients is* $C_{Y_i(t)Y_j(t)} = E[Y_i(t;\omega)Y_j(t;\omega)]$. *The associated boundary conditions have the form*

$$\mathscr{B}[\bar{u}(\xi,t;\omega)]|_{\xi\in\partial D} = E[h(\xi,t;\omega)],$$
$$\mathscr{B}[u_i(\xi,t)]|_{\xi\in\partial D} = E[Y_j(t;\omega)h(\xi,t;\omega)]C^{-1}_{Y_i(t)Y_j(t)},$$

*and the initial conditions for the DO components are given by*

$$\bar{u}(x,t_0) = E[u_0(x;\omega)],$$
$$Y_i(t_0;\omega) = \langle u_0(\cdot,\omega) - \bar{u}(x,t_0), v_i(\cdot)\rangle,$$
$$u_i(x,t_0) = v_i(x),$$

*for all* $i = 1,\dots,n$, *where* $v_i(x)$ *are the eigenfields of the covariance operator* $C_{u(\cdot,t_0)u(\cdot,t_0)}$ *defined by the following eigenvalue problem for* $t = t_0$*:*

$$\int_D C_{u(\cdot,t_0)u(\cdot,t_0)}(x,y)\, v_i(x)dx = \lambda_i(t)\, v_i(y), \quad y \in D. \tag{6}$$

**Remark 1.** The DO evolution Eqs. (5a)–(5c) are derived by using the DO conditions and DO representation. It is shown in [1] that by imposing suitable restrictions on the DO representation the equations for methods such as Polynomial Chaos or Proper Orthogonal Decomposition (POD) can be recovered from the DO evolution equations. For example, PC can be recovered by setting $Y_i(t;\omega) = \Psi_i(\xi(\omega))$, where $\Psi_i(\xi)$ is an orthogonal polynomial in terms of $\xi$.

**Remark 2.** From the DO representation, the moments can be readily computed. For example, the first moment, *i.e.*, the mean, appears in the DO representation as $\bar{u}(x,t)$ while the second moment is directly computed as follows:

$$Var[u] = E[(u-\bar{u})^2] = E\left[\left(\sum_{i=1}^{N} u_i Y_i\right)^2\right] = \sum_{i,j=1}^{N} u_i(x,t)E[Y_iY_j]u_j(x,t).$$

As the DO representation at any fixed time $t$ can be seen as Karhunen–Loeve decomposition, there is a relationship between the eigenpairs for the covariance matrix of $Y_i(t;\omega),\ i = 1,\dots,N$ and the eigenpairs for the covariance operator of $u(x,t;\omega)$. For the covariance matrix $C$ whose $(i,j)$ element is $C_{ij} = C_{Y_i(t)Y_j(t)}$, we have a set of eigenvalues and eigenvectors that satisfies the following eigenvalue problem

$$C(t)\phi_k(t) = \rho_k\phi_k(t), \quad k = 1,\dots,N, \tag{7}$$

where $\phi_k(t) = (\phi_{k1}(t),\dots,\phi_{kN}(t))^T$. Similarly, for the covariance operator for $u(x,t;\omega)$, there exists a set of eigenvalues and eigenfields for $C_u(x,y)$ through the Karhunen–Loeve decomposition such that

$$\int_D C_u(x,y)\, v_k(x,t)dx = \lambda_k\, v_k(y,t), \tag{8}$$

where $C_u(x,y) = E[(u(x,t;\omega) - \bar{u}(x,t))(u(y,t;\omega) - \bar{u}(y,t))]$. In order to relate the eigenvalues and eigenvectors for $Y_i$ with those for $u(x,t;\omega)$, we substitute the DO representation of $u$ into $C_u(x,y)$ and compare Eqs. (7) and (8) to obtain the following relations:

$$\lambda_k = \rho_k; \quad v_k(x,t) = \phi_{kl}(t)u_l(x,t).$$

This shows that the stochastic coefficients $Y_i$ together with the modes $u_i$ provide the necessary information to describe both the shape and magnitude of the uncertainty that characterizes a stochastic field but also the principal directions in $\mathscr{H}$ over which this stochasticity is distributed.

### 2.4. Hybrid method: combining PC with DO

In Theorem 1, it is assumed that the initial condition for the SPDE is random from which the corresponding initial conditions for DO components are derived. However, in practice in many cases the initial condition for the SPDE is deterministic while the randomness comes from other sources such as random coefficients or random forcing. Then $Y_i,\ i = 1,\dots,N$ at the initial time becomes zero, which makes the covariance matrix for $Y_i$ singular. Although the singular limit for the DO equations exist, the transition to finite covariance creates numerical issues. Most importantly, in such a case it is not clear what is the optimal choice to initiate the stochastic subspace. For such problems we propose a hybrid approach of Polynomial Chaos (PC) and DO methods in order to avoid the aforementioned problems. Specifically, for PC we employ the probabilistic collocation method (PCM) or multi-element PCM (ME–PCM), which was found to effectively deal with problems exhibiting low regularity in parametric space as well as for long-term integration [23]. We first use PCM or ME–PCM from the initial time $t_0$

up to some time, say $t_s$, provided that the stochasticity is sufficiently developed, and then switch over to the DO method at $t_s$ and employ the KL decomposition to initialize $\bar{u}, \{Y_i\}$ and $\{u_i\}$.

First, we construct the covariance matrix $C_{u(\cdot,t_s)}(x,y)$

$$C_{u(\cdot,t_s)}(x,y) = E[(u(x,t_s) - \bar{u}(x,t_s))(u(y,t_s) - \bar{u}(y,t_s))],$$

where $u$ and $\bar{u}$ at $t = t_s$ are known from PC computations. Then, we compute the eigenpairs for $C_{u(\cdot,t_s)}(x,y)$ by solving

$$\int_D C_{u(\cdot,t_s)}(x,y)\phi(x)dx = \lambda\phi(y).$$

By setting

$$u_i(x,t_s) = \frac{\phi_i(x)}{\|\phi_i\|} \quad \text{and} \quad Y_i(t_s,\omega) = \langle u(x,t_s;\omega) - \bar{u}(x,t), u_i\rangle,$$

we initialize the DO components at $t = t_s$ and we are ready to solve the DO evolution equations. This procedure is summarized in Algorithm 1.

**Algorithm 1.** Hybrid approach of PC and DO method

1: Run PCM or ME–PCM up to $t = t_s$ from $t = 0$.
2: At $t = t_s$, use the KL decomposition for the solution:

$$u(x,t_s;\omega) = \bar{u}(x,t_s) + \sum_{i=1}^{N} Y_i(t_s;\omega)\phi_i(x,t_s).$$

From the KL decomposition, we can initialize $\bar{u}(x,t_s), \{Y_i(t_s;\omega)\}$ and $\{u_i(x,t_s)\}$ for DO method.
3: Switch over to the DO method up to time $t = t_f$.

We will illustrate how the DO evolution equations are used for solving two SPDEs: (i) advection equation in this section and (ii) Burgers equation in the next section. Both are assumed to have deterministic initial conditions to illustrate the advantages of the proposed hybrid approach.

## 3. Numerical example I: advection equation

Consider the following stochastic advection equation [24]

$$\frac{\partial u}{\partial t} + V(t;\omega)\frac{\partial u}{\partial x} = 0, \quad \forall (t,x) \in [0,T] \times D = [0,2\pi] \tag{9a}$$

$$u(0,x) = g(x) = \sin(x), \quad \forall x \in D \tag{9b}$$

The randomness comes from the advection velocity $V(t;\omega)$, which is considered to be either time-independent or time-dependent. For the time-independent case it is assumed to be a Gaussian random variance $V(t;\omega) = V(\omega) = \xi \sim N(0,\sigma^2)$, while for the time-dependent case a stochastic process whose covariance kernel is given as $C_V(t_1,t_2) = \sigma \exp\left(-\frac{|t_1-t_2|}{L}\right)$, with $L$ being the correlation length. It is known in [24] that the stochastic advection Eq. (9) has exact solutions for the mean and variance.

The random transport velocity is decomposed through the truncated Karhunen–Loeve representation

$$V(t,\omega) = E[V](t) + \sum_{i=1}^{M} \sqrt{\lambda_i}\phi_i(t)Z_i, \tag{10}$$

where $\{Z_i\}_{i=1}^M$ are uncorrelated random variables with zero mean and unit variance, and $\{\phi_i(t),\lambda_i\}_{i=1}^M$ is the eigenpair corresponding to the covariance kernel $C_V(t_1,t_2)$, *i.e.* satisfying

$$\int_D C_V(t_1,t_2)\phi_i(t_2)dt_2 = \lambda_i\phi_i(t_1), \tag{11}$$

where the exponential covariance kernel has a closed form for the eigenfunctions [24]:

$$\phi_i(t) = \frac{w\cos(wt)/c + \sin(wt)}{\sqrt{(1+w^2/c^2)T/2 + (w^2/c^2-1)\sin(2wT)/(4w) + (1-\cos(2wT))/(2c)}}, \tag{12}$$

where $c = 1/L$ and $w = \sqrt{2c/\lambda_i - c^2}$. The theorem of Cameron and Martin [25] guarantees that the truncated decomposition converges to $V$ as $M$ goes to infinity; further, we assume that $E[V](t) = 0$.

Using the DO representation, we obtain the form of the evolution operator $\mathscr{L}$

$$\mathscr{L}(u) = -V(t;\omega)\left(\frac{\partial \bar{u}}{\partial x}(x,t) + \sum_{i=1}^{N} Y_i(t;\omega)\frac{\partial u_i}{\partial x}(x,t)\right).$$

### 3.1. Exact formulas of DO components

In this subsection, we derive the exact formulas of DO components $u_i$ and $Y_i$, $i = 1,\ldots,N$ for the stochastic advection equation. First we consider a *time-independent* case, i.e., $V(t;\omega) = V(\omega) = \xi(\omega)$. The exact solution for Eq. (9) is $u(x,t;\omega) = g(x - V(\omega)t) = \sin(x - \xi t)$ and hence

$$u(x,t;\omega) = \sin(x)\cos(\xi t) - \cos(x)\sin(\xi t). \tag{13}$$

In the DO representation, the solution is expressed as $u(x,t;\omega) = E[u](x,t) + \sum_{i=1}^{N} u_i(x,t)Y_i(t;\omega)$ and comparing this with Eq. (13) yields

$$\sum_{i=1}^{N} u_i(x,t)Y_i(t;\omega) = -\cos(x)\sin(\xi t) + \sin(x)\left(\cos(\xi t) - \exp\left(-\frac{\sigma^2 t^2}{2}\right)\right),$$

where the last term is the mean of the solution. Hence we have a *finite* number of modes, i.e., $N = 2$, and the exact formulas for $u_i$ and $Y_i$ are as follows:

$$u_1(x,t) = \frac{\cos(x)}{\sqrt{\pi}}, \quad u_2(x,t) = \frac{\sin(x)}{\sqrt{\pi}}$$

$$Y_1(t;\omega) = -\sqrt{\pi}\sin(\xi t), \quad Y_2(t;\omega) = -\sqrt{\pi}\left(\cos(\xi t) - \exp\left(-\frac{\sigma^2 t^2}{2}\right)\right).$$

Note that the DO basis is scaled to be an orthonormal basis while the DO components are the same up to the sign, i.e., $\sum_i u_i Y_i = \sum_i (-u_i)(-Y_i)$.

In a similar way we can derive the exact formulas of DO components when $V(t;\omega)$ is *time-dependent* with covariance kernel being $C_V(t_1,t_2) = \sigma^2 \exp\left(-\frac{|t_1 - t_2|}{L}\right)$. We have again $N = 2$ and the exact formulas for $u_i$ and $Y_i$ are:

$$u_1(x,t) = \frac{\cos(x)}{\sqrt{\pi}}, \quad u_2(x,t) = \frac{\sin(x)}{\sqrt{\pi}}$$

$$Y_1(t;\omega) = -\sqrt{\pi}\sin\left(\int_0^t V(s;\omega)ds\right), \quad Y_2(t;\omega) = -\sqrt{\pi}\left(\cos\left(\int_0^t V(s;\omega)ds\right) - \exp\left(-\frac{a^2(t)\sigma^2}{2}\right)\right),$$

so the time-dependent modes are given by semi-analytical forms.

### 3.2. Numerical solution of the evolution equations

The DO evolution Eqs. (5a)–(5c) involve the numerical integration in physical space as well as in random space. We define the collocation points and weights for the physical space by $(x_k, w_k)_{k=1}^{N_s}$ and the random space by $(\xi_j, \gamma_j)_{j=1}^{N_r}$. We choose Fourier collocation points for $x_k$, $k = 1,\ldots,N_s$, and sparse grids based on Gauss–Hermite in one dimension for $\xi_j$, $j = 1,\ldots,N_r$. For the time discretization, we use explicit methods for all DO evolution Eqs. 5a, 5b, 5c. Two inner products are involved in DO equations, given in discrete form below:

- Inner product in the physical space

$$\langle h(x), g(x)\rangle = \int_D h(x)g(x)dx \approx \sum_{k=1}^{N_s} h(x_k)g(x_k)w_k.$$

- Inner product in the random space, i.e., expectation operator

$$E[h(\omega), g(\omega)] = \int_\Omega h(\omega)g(\omega)\rho(\omega)d\omega \approx \sum_{j=1}^{N_r} h(\xi_j)g(\xi_j)\gamma_j.$$

Substituting these equations into the DO Eqs. (5b) yields

$$\begin{aligned}
\frac{dY_i(t;\omega)}{dt} &= \langle \mathscr{L}[u(\cdot,t;\omega)] - E[\mathscr{L}[u(\cdot,t;\omega)]], u_i(\cdot,t)\rangle = \sum_{k=1}^{N_s}(\mathscr{L}(t,x_k) - E[\mathscr{L}(u)](t,x_k))u_i(t,x_k)w_k \\
&= \sum_{k=1}^{N_s}\left(-V(t,\omega)\frac{\partial \bar{u}}{\partial x}(t,x_k) - \sum_{j=1}^{N}\left(V(t,\omega)Y_j(t,\omega) - E[VY_j](t)\right)\frac{\partial u_j}{\partial x}(t,x_k)\right)u_i(t,x_k)w_k \\
&= -B_i V(t,\omega) - V(t,\omega)\sum_{j=1}^{N} Y_j(t,\omega)A_{ji} + \sum_{j=1}^{N} E[VY_j]A_{ji}, \quad i = 1,\ldots,N
\end{aligned}$$

where

$$B_i = \sum_{k=1}^{N_s} \frac{\partial \bar{u}}{\partial x}(t,x_k)u_i(t,x_k)w_k \quad \text{and} \quad A_{ji} = \sum_{k=1}^{N_s} \frac{\partial u_j}{\partial x}(t,x_k)u_i(t,x_k)w_k.$$

Note that for each $i$ the above stochastic differential equation is a vector equation of size $N_r$ because we solve the equation at the collocation points $\xi_j,\ j = 1,\ldots,N_r$. Therefore, there are $N \times N_r$ equations for $Y_i$.

The equation for the mean $\bar{u}$ becomes

$$\frac{\partial \bar{u}(t,x)}{\partial t} = E^{\omega}[\mathscr{L}[u(\cdot,t;\omega)]] = -\sum_{i=1}^{N} E[VY_i](t)\frac{\partial u_i}{\partial x}(t,x)$$

since $E[V](t) = 0$. Note that we solve this equation at the collocation points $x_k,\ k = 1,\ldots,N_s$ and $E[VY_i]$ is independent of the physical space.

The third equation for the modes $u_i(t,x),\ i = 1,\ldots,N$ becomes

$$\sum_{i=1}^{N} C_{ij}\frac{\partial u_i}{\partial t}(t,x) = \prod_{V_s^{\perp}}[E^{\omega}[\mathscr{L}[u(\cdot,t;\omega)]Y_j] = E^{\omega}[\mathscr{L}[u(\cdot,t;\omega)]Y_j] - \sum_{k=1}^{N}\langle E^{\omega}[\mathscr{L}[u(\cdot,t;\omega)]Y_j](t,x), u_k(t,x)\rangle u_k(t,x)$$

where

$$C_{ij} = C_{Y_i(t)Y_j(t)} = E[Y_i(t,\omega)Y_j(t,\omega)] = \sum_{k=1}^{N_r} Y_i(t,\xi_k)Y_j(t,\xi_k)\gamma_k.$$

The term $E[\mathscr{L}[u(\cdot,t;\omega)]Y_j](t,x)$ can be computed as follows:

$$D_{kj} = E[\mathscr{L}[u(\cdot,t;\omega)]Y_j](t,x_k) = -E[VY_j](t)\frac{\partial \bar{u}}{\partial x}(t,x_k) - \sum_{i=1}^{N} E[VY_iY_j](t)\frac{\partial u_i}{\partial x}(t,x_k)$$

### 3.3. Numerical results for time-independent $V(\omega)$

We consider the case where $V(t;\omega)$ is a Gaussian random variable with mean 0 and variance $\sigma^2$. We present two different methods to solve the DO evolution Eqs. 5a, 5b, 5c. In the first we assume that $Y_i(0;\omega) = 0$ and $u_i(x,0)$ are orthogonal polynomials while in the second we use the hybrid method proposed in Section 2.4. The parameters are as follows $\Delta t = 0.001,\ t_f = 5,\ N = 2,\ N_s = 128,\ N_r = 32,\ \sigma = 0.1$, where $t_f$ is the final time. Fourier collocation in the physical space and Hermite collocation in the parametric (or random) space are used to discretize the space. (The number of collocation points in the physical space is denoted by $N_s$ while the number in the random space $N_r$.) We use the third-order Adams–Bashforth (AB3) as a time-integrator to minimize the error due to the time discretization. Indeed, Fig. 1 shows that AB3 is much better than the Euler method with errors approaching machine accuracy. Although this is expected, we want to obtain the absolute errors of time integration so that we will only consider the errors in parametric space later. Also, this temporal accuracy will be very important when we switch from PC to the DO method. The relative $L_2$ error for the mean is defined as $|E(u_{num}) - E(u_{exact})|_{L_2}/|E(u_{exact})|_{L_2}$ where $u_{num}$ is the numerical solution and $u_{exact}$ is the exact solution.

The exact solution, which is used as reference, for the mean and the variance has the closed form [24]:

$$E[u](t,x) = \sin(x)\exp\left(-\frac{\sigma^2 t^2}{2}\right), \quad E[u^2](t,x) = \frac{1}{2}\left[1 - \cos(2x)\exp(-2\sigma^2 t^2)\right], \quad Var[u^2](t,x) = E[u^2] - E[u]^2,$$

where $u(x,t) = g(x-\xi t) = \sin(x-\xi t)$.

#### 3.3.1. DO method with initial basis being orthogonal polynomials

Since the initial condition is deterministic, the stochastic coefficients $Y_i(0;\omega),\ i = 1,\ldots,N$ are zero. To illustrate how the solution evolves in time through the DO evolution equations, we choose initially the linear subspace $V_S$ spanned by orthogonal polynomials with the stochastic coefficients $Y_i$ being zero. The orthogonal polynomials on $[0,2\pi]$ can be constructed using Gram–Schmidt orthogonalization.

Fig. 2 shows how the basis for $V_S$ evolves in time through the DO evolution Eq. (5c). As mentioned, orthogonal polynomials on $[0,2\pi]$ are chosen as a basis for the initial condition for $u_i,\ i = 1,\ldots,N$ and they are evolving and converge to the Fourier basis of period one. Once they become the Fourier basis, the linear subspace $V_S$ does not change but remains invariant in time. The mean and variance are shown in Fig. 3 and they agree well with the exact solution at $t_f = 5$. This shows that the DO method can recover (“on-the-fly”) the optimal basis as it is integrated in time.

#### 3.3.2. Hybrid DO method

The number of DO modes $N$ should be chosen in such a way that the KL decomposition of the solution with $N$ terms approximates well the solution $u(x,t;\omega)$. The switching time from PC to DO is chosen as $t_s = 0.001$. In other words, for this

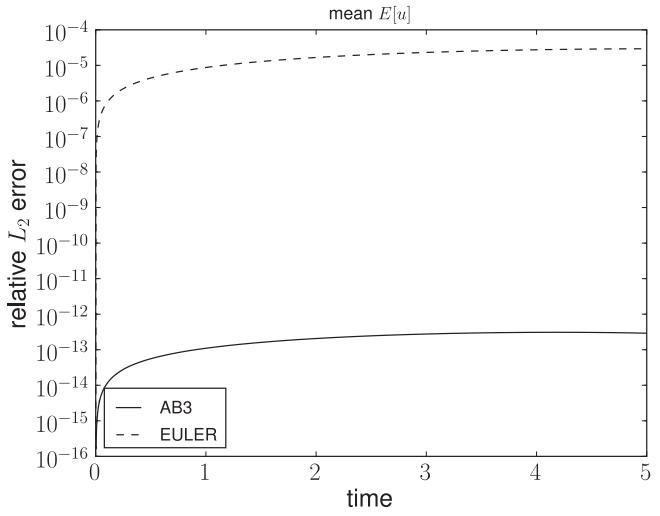


**Fig. 1.** $V(t;w) = V(w) = \xi \sim N(0,\sigma^2)$ with $\sigma = 0.1$. The mean of the solution using AB3 has eight orders of magnitude better accuracy than the Euler method.

simple linear problem only one time step for the probabilistic collocation method may be used to switch over to DO method. The basis from KL decomposition at $t_s = \Delta t$ is, in fact, the Fourier basis so it does not change in time, i.e. the linear subspace does not evolve but remains invariant in time. Fig. 4 shows the mean and variance at $t = 5$ with the hybrid method with $t_s = 0.001$.

We now examine the error of the mean and variance and compare them with those from PCM. Both have the same parameters such as $\Delta t, N_s$ and $N_r$ for numerical discretization. As shown in Fig. 5, DO have as good an accuracy as PCM does for the mean and variance. However, DO are faster than PCM as will be demonstrated in the next subsection. While the error of $u_i$ stays constant in time, the error of $Y_i$ increases in time, hence it accounts for the increase of the error of the variance since the covariance matrix of the stochastic coefficients is involved in the variance.

Since we know the exact formulas for DO components, we can compute the error of DO component computed numerically in Section 3.2, and they are shown in Fig. 6.

### 3.4. Numerical results for time-dependent $V(t,\omega)$

We consider the case where $V(t;\omega)$ is described by the exponential covariance in time, *i.e.* $C_V(t_1,t_2) = \sigma \exp(-\frac{|t_1-t_2|}{L})$ and $L$ is the correlation length that characterizes the stochastic process. The exact solution is $u(x,t;\omega) = \sin\left(x - \int_0^t V(s;\omega)ds\right)$ and its mean and variance are as follows:

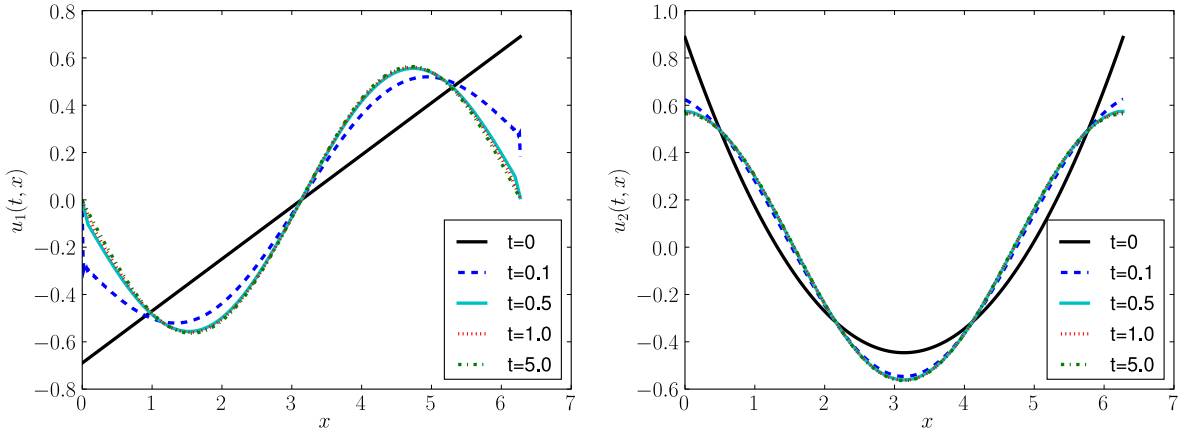


**Fig. 2.** $V(t;w) = V(w) = \xi \sim N(0,\sigma^2)$ with $\sigma = 0.1$. Left: $u_1$, Right: $u_2$. Initially $u_1$ and $u_2$ are polynomials of first and second-degree, respectively. They evolve via the DO evolution equation and change into the Fourier basis. Once they become the Fourier basis, they are invariant.

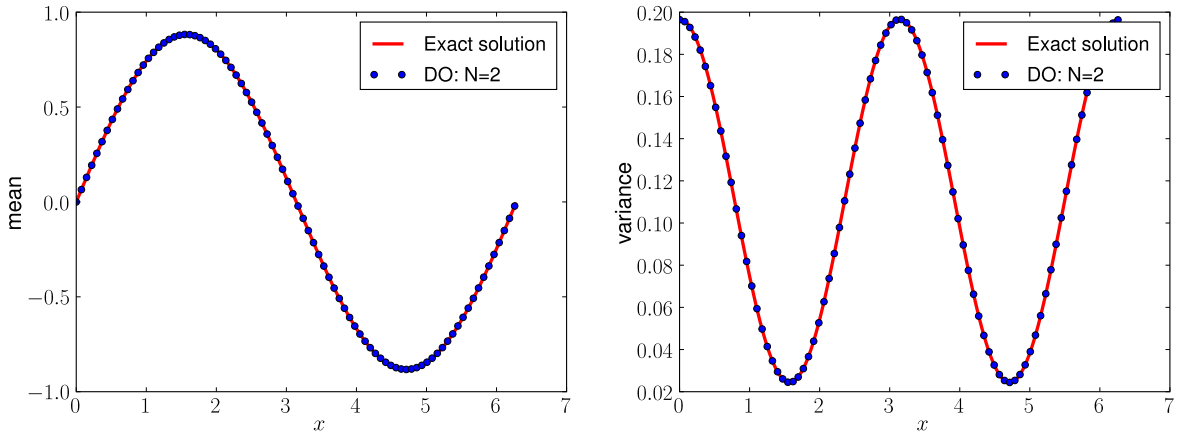


**Fig. 3.** $V(t;w) = V(w) = \xi \sim N(0,\sigma^2)$ with $\sigma = 0.1$. Mean (left) and variance (right) of the advection equation at $t_f = 5$ with the initial condition for $u_i$ being orthogonal polynomials. The parameters are $\sigma = 0.1, N_s = 128$ and $N_r = 32$.

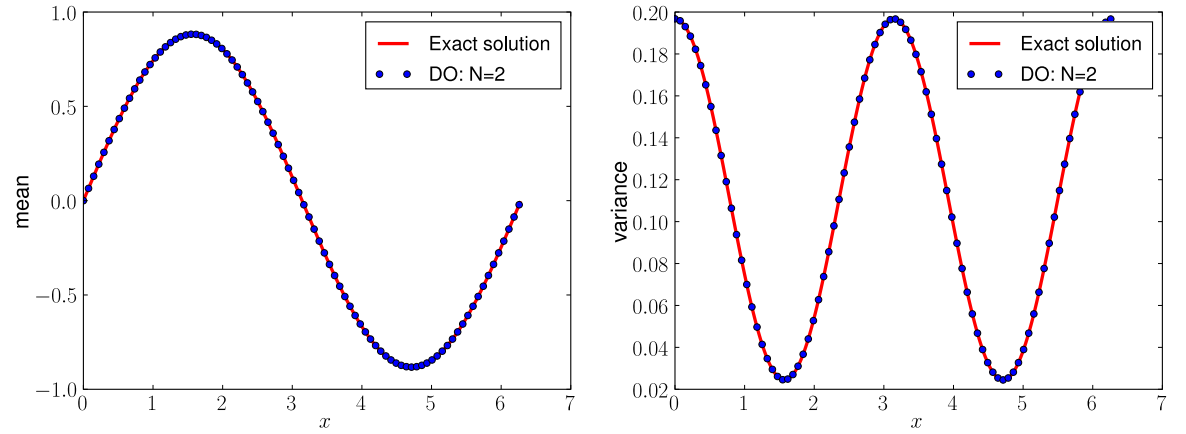


**Fig. 4.** $V(t;w) = V(w) = \xi \sim N(0,\sigma^2)$ with $\sigma = 0.1$. Mean (left) and variance (right) of the advection equation at $t_f = 5$ from hybrid method. They agree well with the exact solution. The parameters are $\sigma = 0.1, N_s = 128$ and $N_r = 32$.

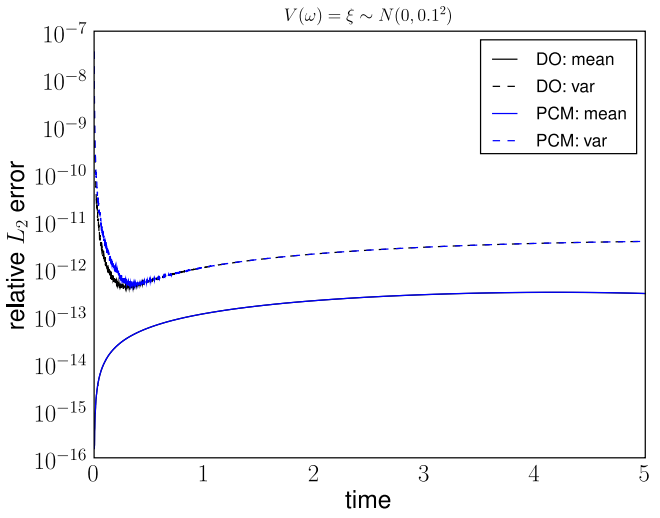


**Fig. 5.** $V(t;w) = V(w) = \xi \sim N(0,\sigma^2)$ with $\sigma = 0.1$. Errors in the mean and variance using DO and PCM are identical.

$$E[u](x,t) = \sin(x - \overline{V}t)\exp(-a^2\sigma^2/2) \tag{14}$$

$$V[u](x,t) = \frac{1 - \cos(2(x-\overline{V}t))\exp(-2\sigma^2a^2)}{2} - E[u]^2, \tag{15}$$

where $a = a(t)$ depends on the type of the process $V(t;\omega)$ we model, i.e.,

$$a^2 = \begin{cases} t^2, & \text{if fully correlated,} \\ 2L(t - L(1-\exp(-t/L))), & \text{partially correlated,} \\ t\Delta t, & \text{mutually independent} \end{cases}$$

The parameters are

$$\Delta t = 10^{-3}, \quad L = 5, \quad \sigma = 0.1, \quad t_f = 5, \quad N_s = 128.$$

We use KL decomposition to discretize $V(t;\omega)$ and the dimension of random space is determined by how many terms in the KL decomposition we keep. Table 1 shows the dimension of the parametric space with respect to the percentage of energy above which we keep the terms. We solve the stochastic advection equation using three methods; one is the hybrid DO method and the other PCM. As we increase the dimensionality of the parametric space by adding more terms in the KL decomposition of $V(t;\omega)$, the error of the mean and variance decreases as shown in Fig. 7. Note that, like the time-independent case, DO and PCM has the same order of magnitude of the error when they use the same parameters for numerical discretization. However, DO are much faster than PCM, especially for high-dimensional parametric space as shown in Fig. 8.

## 4. Numerical example II: Burgers equation

In this section, we consider the Burgers equation. First, assuming that the basis and stochastic coefficients are known exactly, we obtain the proper forcing in the Burgers equation from which we illustrate convergence. Second, we consider the Burgers equation with random forcing and demonstrate convergence with respect to the number of DO modes.

### 4.1. Case A: exact DO components

We first consider the basis to be periodic in space and time, given by the expression

$$u_n(x,t) = \frac{1}{\sqrt{\pi}}\cos(nx - c_n t), \quad x \in [0, 2\pi], \quad n = 1, 2, \ldots, c_n \in \mathbb{R}.$$

Then, we have the dynamic orthogonality condition, i.e.,

$$\left\langle \frac{\partial u_n}{\partial t}, u_m \right\rangle = 0 \quad \text{and} \quad \langle u_n, u_m \rangle = \delta_{nm}.$$

For the stochastic coefficients, we consider

$$Y_i(t;\omega) = R_i\left(1 - e^{-t/T_i}\right)\cos(\lambda_i t + \varphi_i(\omega)) + \xi_i(\omega), \tag{16}$$

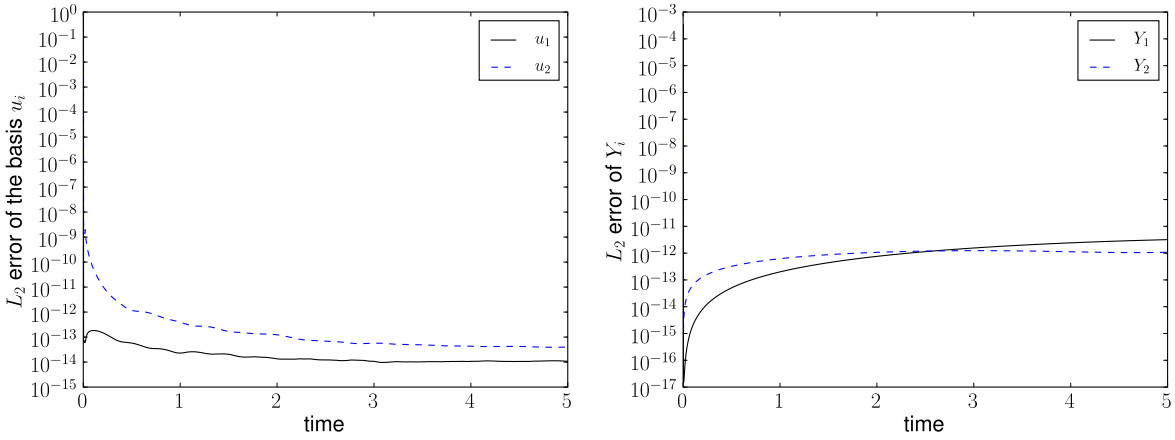


**Fig. 6.** $V(t;w) = V(w) = \xi \sim N(0,\sigma^2)$ with $\sigma = 0.1$. The error of DO components $u_i$ (left) and $Y_i$ (right), $i = 1, 2$. The error for $Y_i$ increases in time, and it accounts for the increase of the error of the variance.

**Table 1**
Dimension (or number of terms in the KL decomposition) of the parametric space with respect to energy.

| Energy (%) | Dimension ($M$) |
|---|---|
| 95 | 5 |
| 99 | 18 |
| 99.9 | 68 |

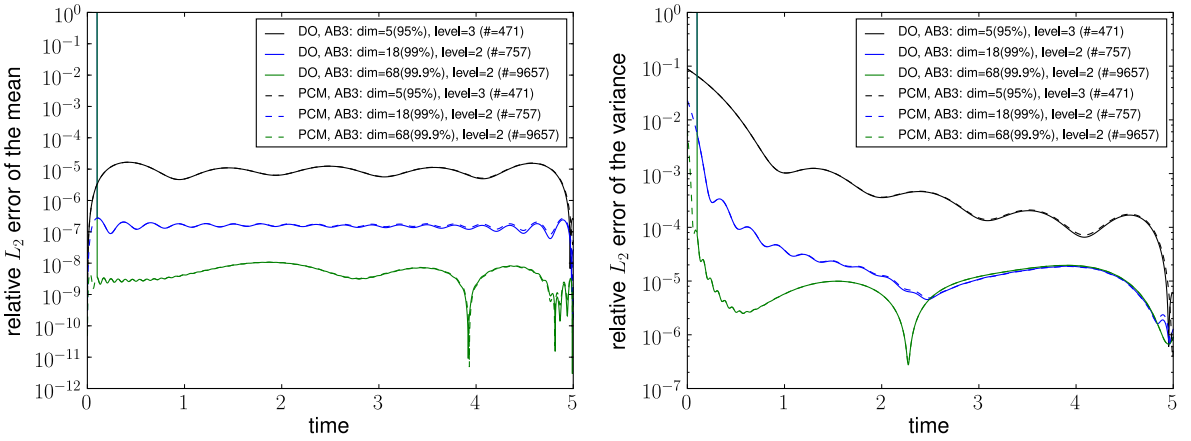


**Fig. 7.** Relative $L_2$ error for the mean (left) and variance (right). The reference solution for the mean and variance is from the exact formula. As we increase the dimension of the random space i.e. we approximate $V(t;\omega)$ better with more terms, the relative $L_2$ error decreases.

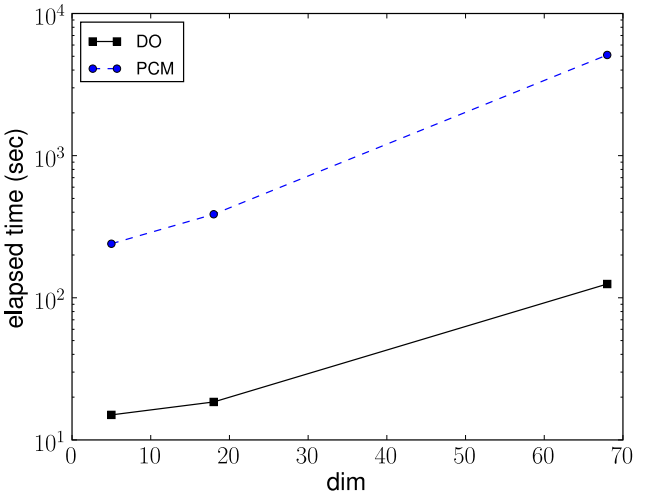


**Fig. 8.** Computational time to solve the advection problem using DO and PCM. DO is much faster than PCM, especially in high dimensions.

where $\xi_i(\omega)$ is a Gaussian random variable with mean zero and variance $\rho_i^2 R_i^2$, and $\varphi_i(\omega)$ is a uniform distribution in $[0, 2\pi]$, $T_i$ and $\lambda_i$ are timescales, and $R_i$ are given positive quantities defining the magnitude of the stochastic coefficient.

By construction we can check that $E^\omega[Y_i(t;\omega)] = 0$, and moreover, for $i \neq j$, $E^\omega[Y_i(t;\omega)Y_j(t;\omega)] = 0$ while, for $i = j, E^\omega[Y_i(t;\omega)Y_j(s;\omega)] = R_i^2[\rho_i^2 + \frac{1}{2}(1 - e^{-t/T_i})(1 - e^{-s/T_i})\cos[\lambda_i(t-s)]]$.

For $t = 0$, we have $Y_i(t;\omega)|_{t=0} = \xi_i(\omega)$, i.e., the stochastic coefficients are normally distributed while, for large $t$, we have that

$$Y_i(t;\omega) = R_i \cos(\lambda_i t + \varphi_i(\omega)) + \xi_i(\omega)$$

since $1 - e^{-t/T_i} \approx 1$.

Based on this form with mean zero field, we have the random field

$$u(x,t;\omega)=\sum_{n=1}^{N}\frac{1}{\sqrt{\pi}}\left(R_n\left(1-e^{-t/T_n}\right)\cos\left(\lambda_n t+\varphi_n(\omega)\right)+\xi_n(\omega)\right)\cos\left(nx-c_n t\right) \tag{17}$$

and the Burgers equation

$$\frac{\partial u}{\partial t}+\frac{\partial u}{\partial x}u-\nu\frac{\partial^2 u}{\partial x^2}=F(x,t;\omega), \tag{18}$$

where the corresponding forcing is given by

$$\begin{aligned}F(x,t;\omega)=&\sum_{n=1}^{N}\frac{R_n}{\sqrt{\pi}}\left(\frac{1}{T_n}e^{-t/T_n}\cos\left(\lambda_n t+\varphi_n(\omega)\right)-\lambda_n\left(1-e^{-t/T_n}\right)\sin\left(\lambda_n t+\varphi_n(\omega)\right)\right)\cos\left(nx-c_n t\right)\\&+\sum_{n=1}^{N}\frac{c_n}{\sqrt{\pi}}Y_n(t;\omega)\sin\left(nx-c_n t\right)-\sum_{n=1}^{N}\sum_{m=1}^{N}\frac{m}{\pi}Y_n(t;\omega)Y_m(t;\omega)\cos\left(nx-c_n t\right)\sin\left(mx-c_m t\right)\\&+\nu\sum_{n=1}^{N}\frac{n^2}{\sqrt{\pi}}Y_n(t;\omega)\cos\left(nx-c_n t\right).\end{aligned}$$

*4.1.1. PDF of $Y_i$ and the solution*

We can derive the exact formula of the probability density function (PDF) of the stochastic coefficients in Eq. (16) and hence the solution $u(x,t;\omega)$. For simplicity, we consider $N=1$ but it can be extended easily to the case with many dimensions. We need the following two lemmas [26].

**Lemma 2.** *Let $X,Z$ be two $\mathscr{R}$-valued independent random variables and let $Y=X+Z$. If $X$ and $Y$ has a density $f_X$ and $f_Z$, respectively, then the PDF of $Y$ is the convolution of $f_X$ and $f_Z$:*

$$f_Y(y)=\int f_X(z-y)f_Z(z)dz=\int f_X(x)f_Z(y-x)dx. \tag{19}$$

**Lemma 3.** *Let $S\in\mathscr{R}^n$ be partitioned into disjoint subsets $S_0,S_1,\ldots,S_m$ such that $\cup_{i=0}^{m}S_i=S$, and such that $m_n(S_0)=0$ where $m_n$ is a Lebesgue measure on $(\mathscr{R}^n,\mathscr{R}^n)$, and that for each $i=1,\ldots,g:S_i\to\mathscr{R}^n$ is injective and continuously differentiable with non-vanishing Jacobian. Let $Y=g(X)$, where $X$ is an $\mathscr{R}^n$-valued random variable with values in $S$ and with density $f_X$. Then, $Y$ has a density given by*

$$f_Y(y)=\sum_{i=1}^{m}f_X(g_i^{-1}(y))|detJ_{g_i^{-1}}(y)| \tag{20}$$

*where $g_i^{-1}$ denotes the inverse map $g_i^{-1}:g(S_i)\to S_i$ and $J_{g_i^{-1}}$ is its corresponding Jacobian matrix.*

Let $\Theta=\varphi, X=\xi\sim N(0,\sigma^2), Z=a(t)\cos(\lambda t+\Theta)=g(\Theta)$ and $Y=X+Z$ with $\sigma=R\rho$ and $a(t)=R(1-\exp(-t/T))$. First, we compute the PDF of $Z$ using Lemma 3. We can decompose $S=[0,2\pi]=S_1\cup S_2$, where $S_1=[0,\pi]$ and $S_2=[\pi,2\pi]$. Since $\Theta$ is a uniform distribution on $S_1\cup S_2$ and $g(\theta)$ is identical on $S_1$ and $S_2$ (up to sign), we only need to consider the domain $S_1$ to compute the PDF of $Z$. The phase does not affect the PDF of $Z$ and hence, in this case $\lambda t$ can be omitted to compute PDF of $Z$, i.e., $f_Z=f_{a(t)\cos(\Theta)}$. Note that

$$\begin{aligned}&f_\Theta(\theta)=\frac{1}{\pi},\quad\text{for}\quad\theta\in S_1\\&g^{-1}(z)=\arccos(z),\quad J_{g^{-1}}(z)=-\frac{1}{\sqrt{1-z^2}}\quad\text{for}\quad z\in[0,\pi],\end{aligned}$$

which gives us

$$f_Z(z)=\frac{1}{a\pi\sqrt{1-(z/R)^2}}.$$

Now we use Lemma 2 to derive the exact PDF of $Y$:

$$\begin{aligned}f_Y(y)&=\int_{-a}^{a}f_X(y-w)f_Z(w)dw=\int_{-a}^{a}\frac{1}{\sqrt{2\pi\sigma^2}}\exp\left(-\frac{(y-w)^2}{2\sigma^2}\right)\frac{1}{a\pi\sqrt{1-(w/a)^2}}dw\\&=\int_{-1}^{1}\frac{1}{\sqrt{2\pi\sigma^2}}\exp\left(-\frac{(y-aw)^2}{2\sigma^2}\right)\frac{1}{\pi\sqrt{1-w^2}}dw=\frac{1}{\pi\sigma\sqrt{2\pi}}\int_0^{\pi}\exp\left(-\frac{(y-a\cos(x))^2}{2\sigma^2}\right)dx\end{aligned} \tag{21}$$

where the third and fourth equality follows from the change of variables. The integration in Eq. (21) can be computed with high accuracy using Gaussian quadrature points since the integrand is smooth.

We can derive the exact PDF of the solution $u(x,t;\omega)$ at $x$ and time $t$ by using Lemma 3 applied to $f_Y(y)$ because $u$ is the multiplication of $Y_1$ by $u_1(x,t)$ that is a constant at fixed $x$ and $t$. Hence, for a fixed $x$ and $t$, the exact PDF of the solution is as follows:

$$f_u(\omega) = \frac{1}{A} f_Y\left(\frac{1}{A}\omega\right), \tag{22}$$

where $A = \frac{1}{\sqrt{\pi}}\cos(x - c_1 t)$. This result can be also verified numerically.

*4.1.2. Computational results*

The stochastic coefficients $Y_1$ depends on a number of parameters which determine the PDF. Here we study two different cases as shown in Table 2.

Initially $Y_1$ is a Gaussian random variable with mean zero and variance $\rho^2 R^2$ but as time goes on, a uniform distribution is introduced through the trigonometric function in Eq. (16) and hence, the PDF of $Y_1$ changes depending on the parameters. For case I and II, the PDF at time $t = 0$ and $t = 1$ is shown in Fig. 9. For case I, the PDF follows the form of Gaussian PDF in time while, for case II, the PDF becomes bimodal so that it has two peaks whose value is far away from zero.

We solve the corresponding Burgers equation using the DO method and estimate the PDF of the stochastic coefficients and the solution at different times and compare them with exact PDF from Eqs. (21) and (22). The parameters for numerical discretization are as follows:

$$\Delta t = 0.001, \quad t_f = 1, \quad N = 1, \quad N_s = 128, \quad N_r = 16,$$

where $N_r$ is the number of collocation points in one-dimension, and a tensor product representation is employed for the numerical discretization in the parametric space as the dimension of the parametric space, in this case 2 since we have two random variables for $Y_1$, is low.

Fig. 10 shows the PDF of the stochastic coefficient and the solution at three different times $t = 0.1, 0.3$, and $1.0$. The PDF of the stochastic coefficient maintains the Gaussian form in time with the variance being widened. Fig. 11 shows the PDF of the stochastic coefficient and the solution at three different times $t = 0.1, 0.2$, and $1.0$. The PDF of $Y$ becomes non-Gaussian and has two peaks whose distance is increasing in time. The plots demonstrate that the DO method is able to capture both Gaussian and non-Gaussian behavior well.

DO and PCM are employed to compute the Burgers equation for comparison, and the $L_2$ errors of the mean and variance are shown in Fig. 12. The same parameters are used for both DO and PCM and the errors are almost identical. Next, we compare the computational efficiency. In the advection equation where the dimension of the parametric space is high, we showed that DO is much faster than PCM in Fig. 8. The computational times with respect to the number of points in the parametric space are shown in Fig. 13; DO is faster than PCM for this problem that has a low dimensional parametric space while the accuracy for both DO and PCM remains the same.

*4.2. Case B: random forcing*

Consider the following stochastic Burgers equation with random forcing

$$\begin{aligned} &\frac{\partial u}{\partial t} + u\frac{\partial u}{\partial x} = \nu\frac{\partial^2 u}{\partial x^2} + \frac{1+\xi}{2}\sin(2\pi t), \quad \forall (t,x) \in [0,T]\times D = [0,2\pi] \\ &u(0,x) = g(x), \quad \forall x \in D, \end{aligned} \tag{23}$$

where $\xi \sim U[-1,1]$ and the initial condition $g(x)$ is given as

$$g(x) = 0.5(\exp(\cos(x)) - 1.5)\sin(x + 2\pi\cdot 0.37). \tag{24}$$

We take $\nu = 0.05$. Note that the period of the forcing is one. Using the DO representation, we obtain the form of the evolution operator $\mathscr{L}$ and some necessary forms:

**Table 2**
Two different cases of parameters for $Y_1$.

| | Case I | Case II |
|---|---|---|
| $T$ | 0.1 | 0.1 |
| $\lambda$ | 1 | 1 |
| $R$ | 0.1 | 0.1 |
| $\rho$ | 1 | 0.1 |

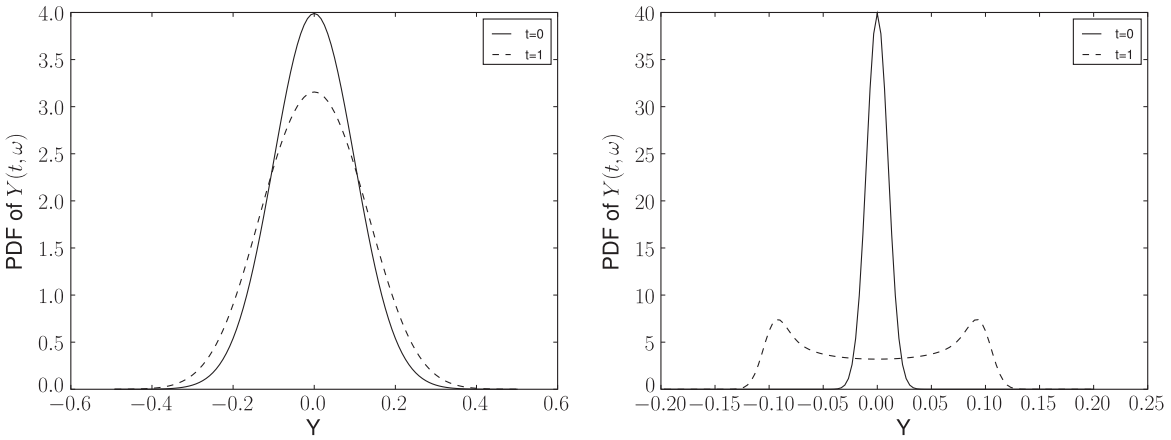


**Fig. 9.** Case I (left) and case II (right). The PDF at $t = 0$ for both cases is Gaussian but as time goes on, the PDF for case II is bimodal while the PDF for case I remains Gaussian with larger variance.

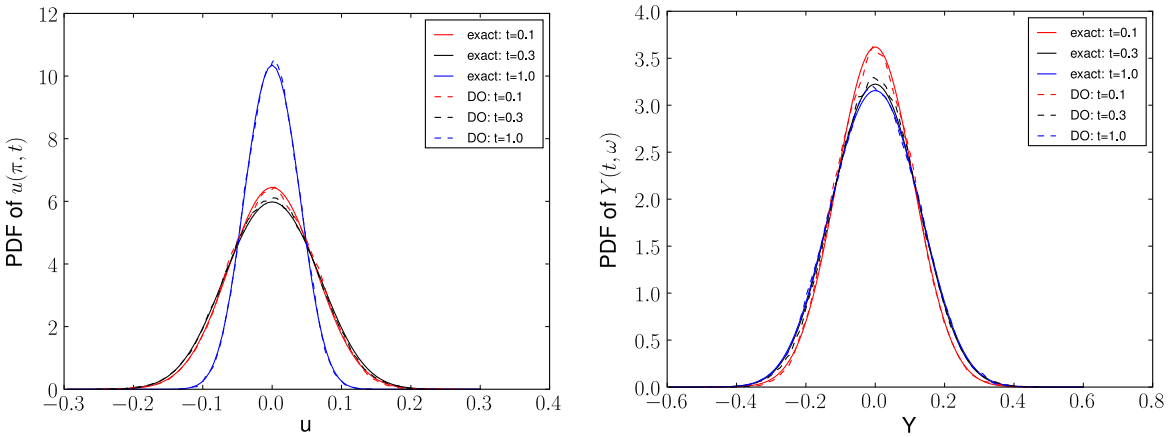


**Fig. 10.** Case I. The PDF of the solution at $x = \pi$ (left) and the stochastic coefficient (right). The PDF maintains the Gaussian form at time $t = 1$, and DO is able to capture the PDF of the solution as well as the stochastic coefficients well.

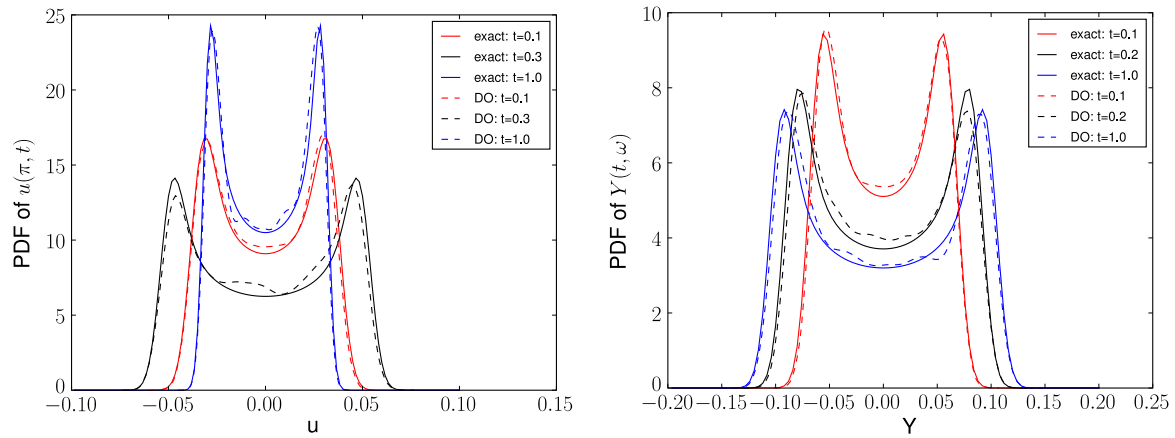


**Fig. 11.** Case II. The PDF of the solution at $x = \pi$ (left) and the stochastic coefficient (right). The PDF evolves from Gaussian to non-Gaussian form, and DO is able to capture this behavior well.

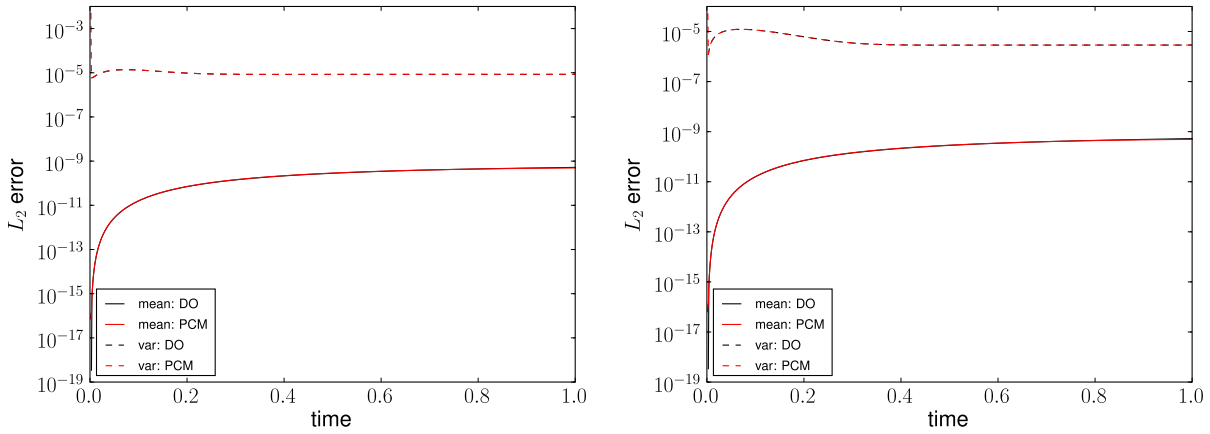


**Fig. 12.** $L_2$ error of the mean and variance for case I (left) and case II (right). For both, DO and PCM exhibit the same accuracy.

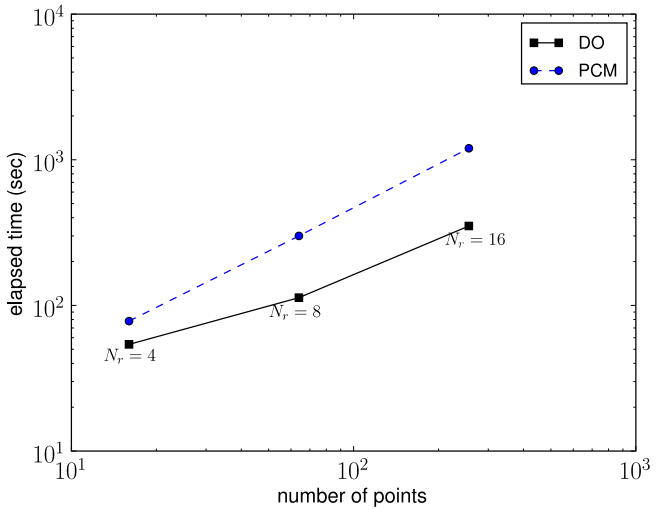


**Fig. 13.** Computational time for PCM and DO. All parameters are the same for both PCM and DO. The number of the collocation points in one direction is denoted by $N_r$. Hence the total number of collocation points are $N_r^2$ since the dimension is 2 and tensor product is used. DO is faster than PCM while the accuracy for both methods is the same.

$$\mathscr{L}[u(x,t;\omega)] = -uu_x + \nu u_{xx} + \frac{1+\xi}{2}\sin(2\pi t) = -\bar{u}\bar{u}_x - Y_i\frac{\partial}{\partial x}(u_i\bar{u}) - Y_iY_ju_i\frac{\partial u_j}{\partial x} + \nu\left(\bar{u}_{xx} + Y_i\frac{\partial^2 u_i}{\partial x^2}\right) + \frac{1+\xi}{2}\sin(2\pi t)$$

$$E[\mathscr{L}(u)] = -\bar{u}\bar{u}_x - C_{ij}u_i\frac{\partial u_j}{\partial x} + \nu\bar{u}_{xx} + 0.5\sin(2\pi t)$$

$$E[\mathscr{L}(u)Y_j] = -\left(C_{ij}u_i\bar{u}_x + C_{kj}\frac{\partial u_k}{\partial x}\bar{u} + C_{ikj}u_i\frac{\partial u_k}{\partial x}\right) + \nu C_{ij}\frac{\partial^2 u_i}{\partial x^2} + E\left[\frac{\xi}{2}Y_j\right]\sin(2\pi t),$$

where $C_{ijk} = E[Y_iY_jY_k]$. Note that $E[\mathscr{L}(u)Y_j]$ involves the third moment of the stochastic coefficients and hence the PDE for $u_i$ is more complicated than the one in the advection equation in the previous section. Since the initial condition is deterministic as in the advection equation, the $Y_i,\ i = 1,\ldots,N$ at the initial time become zero, which makes the covariance matrix for $Y_i$ singular. Hence, we use the *hybrid method* to avoid the singularity due to the deterministic initial condition.

#### *4.2.1. Computational results: hybrid method*

Unlike the advection problem where only one time step is enough to switch from PC to DO, we need to march for more time steps to allow the stochasticity of the system to develop fully. We have performed some sensitivity studies to see how to choose the switching time from PC to DO but a more systematic future study is required. We can choose the number of modes at the switching time based on the eigenvalues of $C_{u(\cdot,t_s)}(x,y)$. One criterion is to choose the number of modes such that the sum of corresponding eigenvalues makes up to more than a threshold, say 99% of the total.

The eigenvalues of KL decomposition of the solution at ten different times are shown in Fig. 14. Note that the eigenvalues of KL decomposition are the same as those of the covariance matrix $C$ whose $(i,j)$ index is $E[Y_iY_j]$. We choose the switching time to be $t_s = 1.0$ and the number of DO modes to be 6 based on Fig. 14. Note that the number of modes should be increased to capture the same percentage of the energy as the system evolves in time.

The parameters are as follows:

$$\Delta t = 0.001, \quad t_s = 1, \quad t_f = 5, \quad N_s = 128, \quad N_r = 64, \quad N = 6.$$

We choose $N = 6$ because, at $t_s = 1$, the sixth mode is the largest eigenmode whose eigenvalue is larger than the threshold value. Fourier collocation in the physical space and Legendre–Gauss collocation in the parametric space are used for discretization. The third-order Adams–Bashforth (AB3) is used as a time integrator to minimize the error due to the time discretization.

The mean and variance at $t = 5$ using the hybrid method are shown in Fig. 15; good agreement with the exact solution is achieved. The $L_2$ error for the mean and variance are shown in Fig. 16.

If the number of modes $N$ is chosen to be smaller than 6, then the KL decomposition with $N$ at the switching time $t_s = 1$ approximates poorly the solution, and hence DO with less number of modes yields larger truncation error. Fig. 17 shows the exponential convergence obtained with respect to the number of modes at time $t = 5$. There is saturation when the number of modes is increased from five to six. This is because the evolution equations for the stochastic coefficients $Y_i$, in particular the fifth and sixth are stiff. The stiffly stable scheme will be required to overcome saturation. This example is the first demonstration of the fast convergence of the DO method for a nonlinear SPDE.

The hybrid DO method is sensitive to the number of modes $N$ and switching time $t_s$ as shown in Fig. 18. The switching time determines the maximum number of possible modes because the DO components are chosen from KL decomposition of the solution at $t_s$. Hence we choose the number of modes to be the largest eigenmode at a given $t_s$. Choosing the switching time is problem-dependent; for the advection equation (linear), we need just one time step to switch over to DO while for the Burgers equation (nonlinear), we need many more time steps for DO to have a good accuracy.

A high-order time discretization for both PCM and DO in the hybrid method is used to minimize the error due to temporal discretization. Fig. 19 shows the relative $L_2$ error for the mean using different time discretization methods for PCM; one is the fourth-order Runge–Kutta (RK4) and the other the third-order Adams–Bashforth (AB3) which is used as a time discretization for the DO method. A large jump at the switching time $t_s = 1$ is observed when the order for the time discretization method is reduced from the fourth-order to the third-order. In this paper, we consider the third-order AB method for DO as well as PCM for the Burgers equation. Hence, compatibility in the temporal accuracy between PCM and DO is required to avoid large error due to switching methods.

## 5. Numerical example III: nonlinear diffusion equation

In this section, we consider the nonlinear diffusion equation which is 1-D in physical space but multi-D in parametric space:

$$\frac{\partial u(t,x)}{\partial t} = \frac{\partial}{\partial x}\left(a(x;\omega)\frac{\partial u(t,x)}{\partial x}\right) + 1, \quad x \in (0,1), \tag{25}$$

$$u(t,0) = u(t,1) = 0, \tag{26}$$

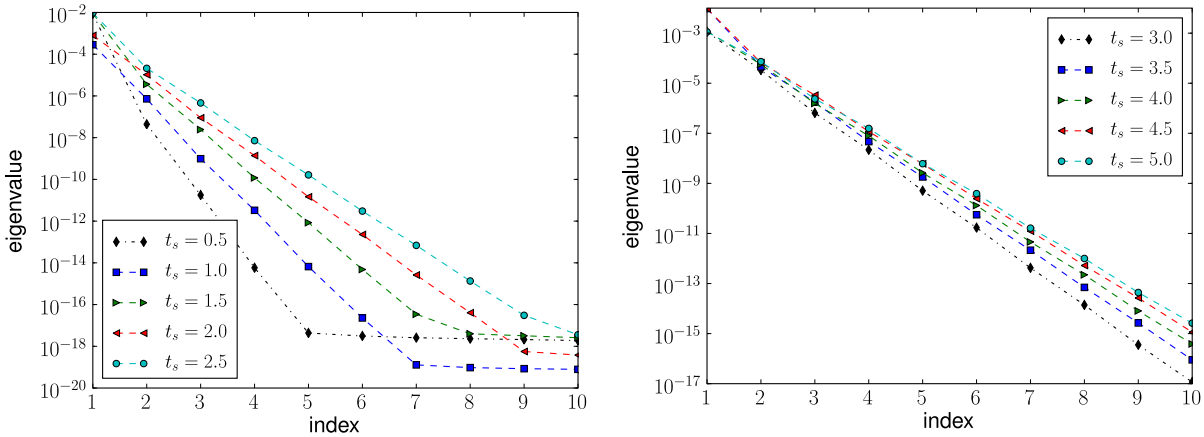


**Fig. 14.** The eigenvalues of the covariance matrix $C$ whose $(i,j)$ index is $E[Y_iY_j]$ at different switch times $t_s$. Left: eigenvalues for $t_s = 0.5j,\ j = 1,\ldots,5$, Right: eigenvalues for $t_s = 0.5j,\ j = 6,\ldots,10$. The parameters used are $\nu = 0.05, N_s = 128, N_r = 64$ and $\Delta t = 0.001$.

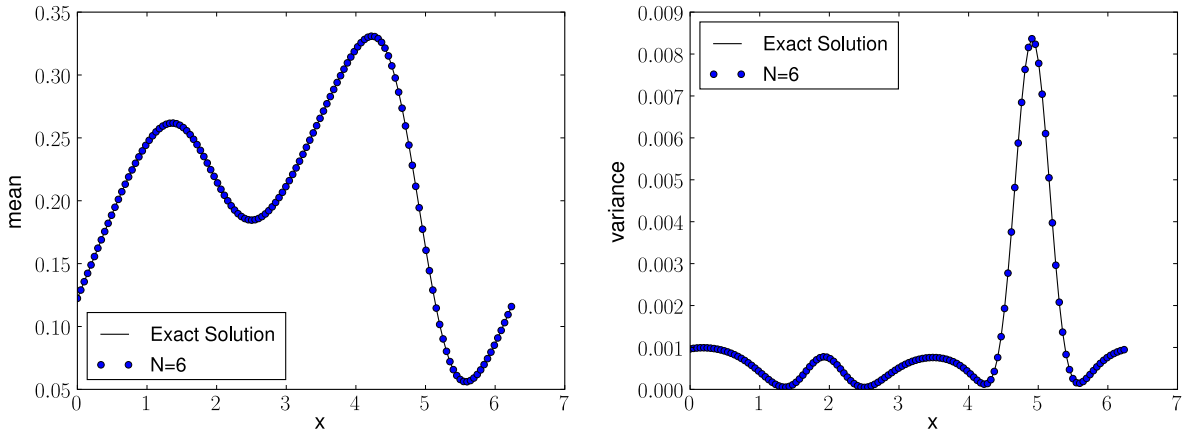


**Fig. 15.** Mean (left) and variance (right) of the solution at $t = 5$ for the Burgers equation. The switching time $t_s$ is 1 and the number of DO modes is 6. The mean and variance from the probabilistic collocation method with $N_r = 512$ using the fourth-order Runge–Kutta method are considered to be the *exact* solution.

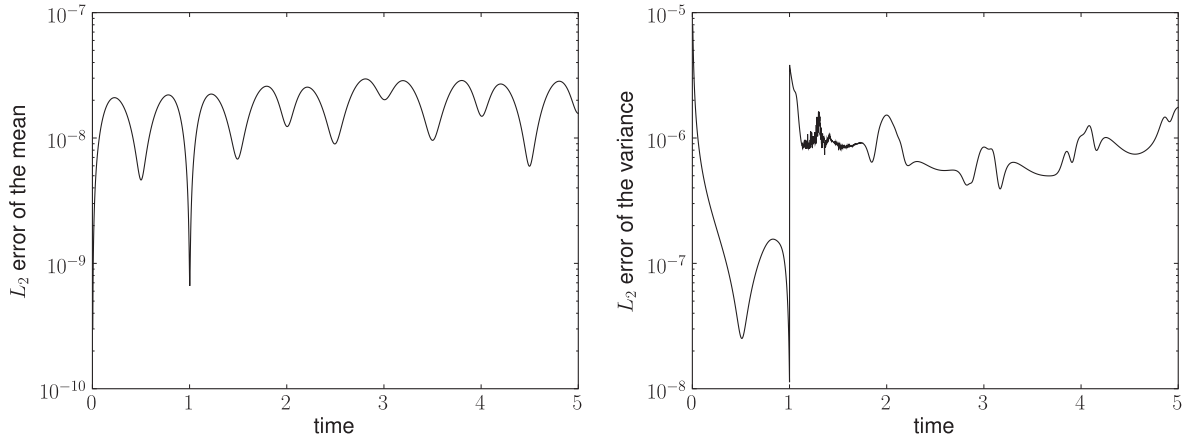


**Fig. 16.** Relative $L_2$ error for the mean (left) and variance (right) of the solution for the Burgers equation with random forcing. The switching time $t_s$ is 1 and the number of DO modes is 6. Since the period of the random forcing is one, the $L_2$ error of the mean also shows periodicity with the same period.

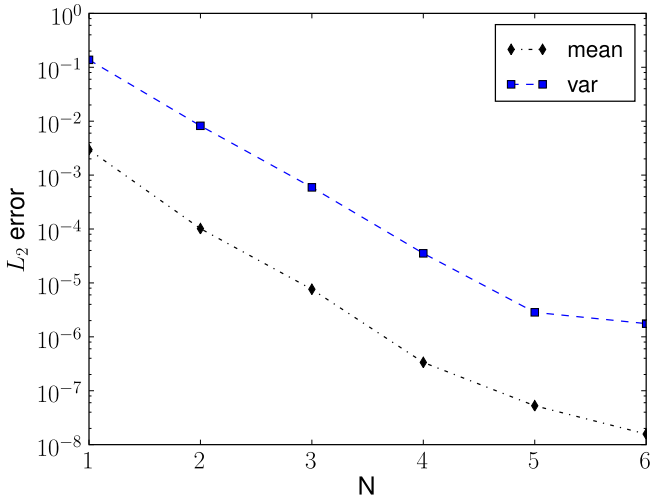


**Fig. 17.** Relative $L_2$ error for the mean and variance at $t = 5$. Exponential convergence is observed as the number of modes increases.

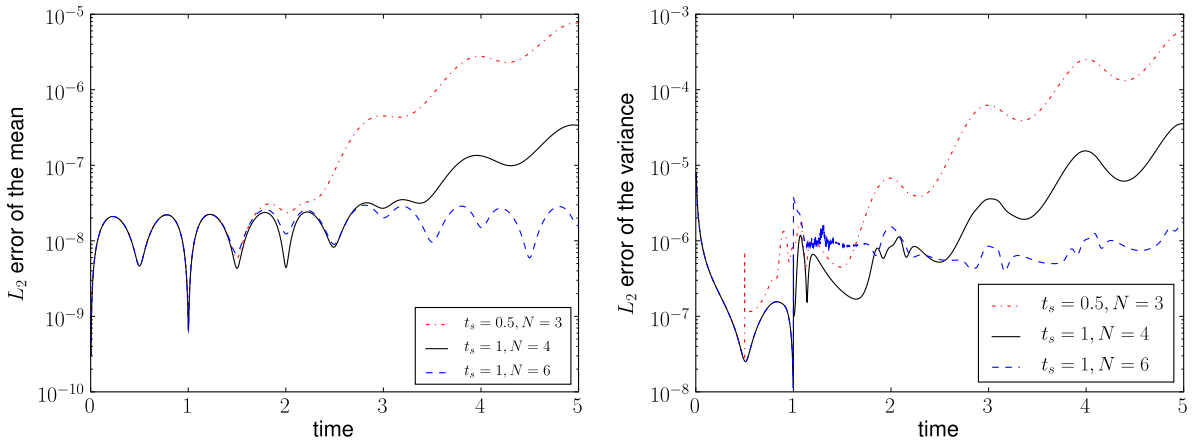


**Fig. 18.** Relative $L_2$ error for the mean (left) and variance (right) of the solution for the Burgers equation. The mean error for $t_s = 0.5$ and $N = 3$ are as good as one for other parameters up to $t = 1.7$ and starts to deviate. $t_s = 1$ and $N = 6$ are shown to be the best among the three cases.

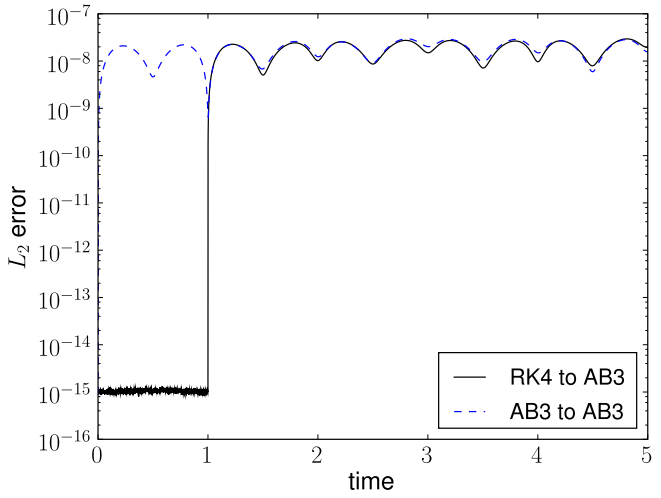


**Fig. 19.** Relative $L_2$ error of the mean for the Burgers equation. Two time discretization methods for PCM are used; black and blue line uses the fourth-order RK and the third-order AB method, respectively. Other parameters for both methods are set to be the same. When the order of the time discretization method is reduced at the switching time, the error increases dramatically.

where the stochastic diffusion coefficients $a(x;\omega)$ is given by the KL expansion

$$a(x;\omega) = \bar{a} + \sigma_a \sum_{i=1}^{M} \sqrt{\lambda_i}\phi_i(x)\xi_i(\omega). \tag{27}$$

$\{\lambda_i\}_{i=1}^{M}$ and $\{\phi_i(x)\}_{i=1}^{M}$ are, respectively, $M$ largest eigenvalues and corresponding eigenfunctions of the Gaussian covariance kernel

$$C_{aa}(x_1, x_2) = \exp\left(-\frac{(x_1 - x_2)^2}{l_c^2}\right), \tag{28}$$

where $l_c$ is the correlation length of $a(x;\omega)$ that dictates the decay of the spectrum of $C_{aa}$. The random variables $\{\xi_i(\omega)\}_{i=1}^{M}$ are assumed to be independent and uniformly distributed on $[-1, 1]$. The coefficient $\sigma_a$ controls the variability of $a(x;\omega)$, and we consider two cases: (i) $l_c = 1, M = 4$ and (ii) $l_c = 1/5, M = 14$ with $\bar{a} = 0.1, \sigma_a = 0.03$. The dimension of random space is determined by how many terms we keep in the KL decomposition of Eq. (27). Using the DO representation, we obtain the form of the evolution operator $\mathscr{L}$:

$$\mathscr{L}[u] = \frac{\partial}{\partial x}\left(a(x;\omega)\frac{\partial \bar{u}}{\partial x}\right) + \sum_i Y_i \frac{\partial}{\partial x}\left(a(x;\omega)\frac{\partial u_i}{\partial x}\right) + 1.$$

A spectral element method was employed for physical space [27] and PCM for parametric space [20] to solve the corresponding DO equations. In particular, we use sparse grids method with Clenshaw–Curtis abscissas because the dimension of random space is modestly high. The reference solution is obtained by PCM with level 5 sparse grids for $M = 14$ and level 6 sparse grids for $M = 4$.

The parameters are

$$\Delta t = 10^{-4}, \quad t_s = 0.5, \quad t_f = 30. \tag{29}$$

We use the forward Euler as a time-integrator with small time step. For DO representation we test different number of modes; for $M = 4$, $N = 1, 2, 3, 4$ and for $M = 14$, $N = 2, 4, 6$ based on the eigenspectrum of the KL decomposition of the solution. The mean and variance at $t = 30$ using the hybrid method are shown in Fig. 20 for $l_c = 1$ and $l_c = 1/5$. Good agreement for higher modes with the exact solution is achieved. Fig. 21 shows the exponential convergence obtained with respect to the number of modes at time $t = 30$.

## 6. Summary

We have developed a hybrid DO-PC method to tackle the singular limit of the DO equations for deterministic initial conditions. In particular, we have presented an efficient approach to deal with the singularity of the stochastic coefficients and the initialization of the DO stochastic subspace. This scheme is based on the solutions of the SPDE in the very initial regime using the Polynomial Chaos method up to the switching time when the stochasticity is developed (obtaining non-Gaussian characteristics) and then switch over to DO method as in Algorithm 1.

We first compared the performance of the two methodologies, i.e. PC and DO methods in analytical examples involving linear and nonlinear problems. In particular, we derived exact formulas of the stochastic coefficients and basis elements for the advection equation and also derived the probability density function of the stochastic coefficients and basis for the

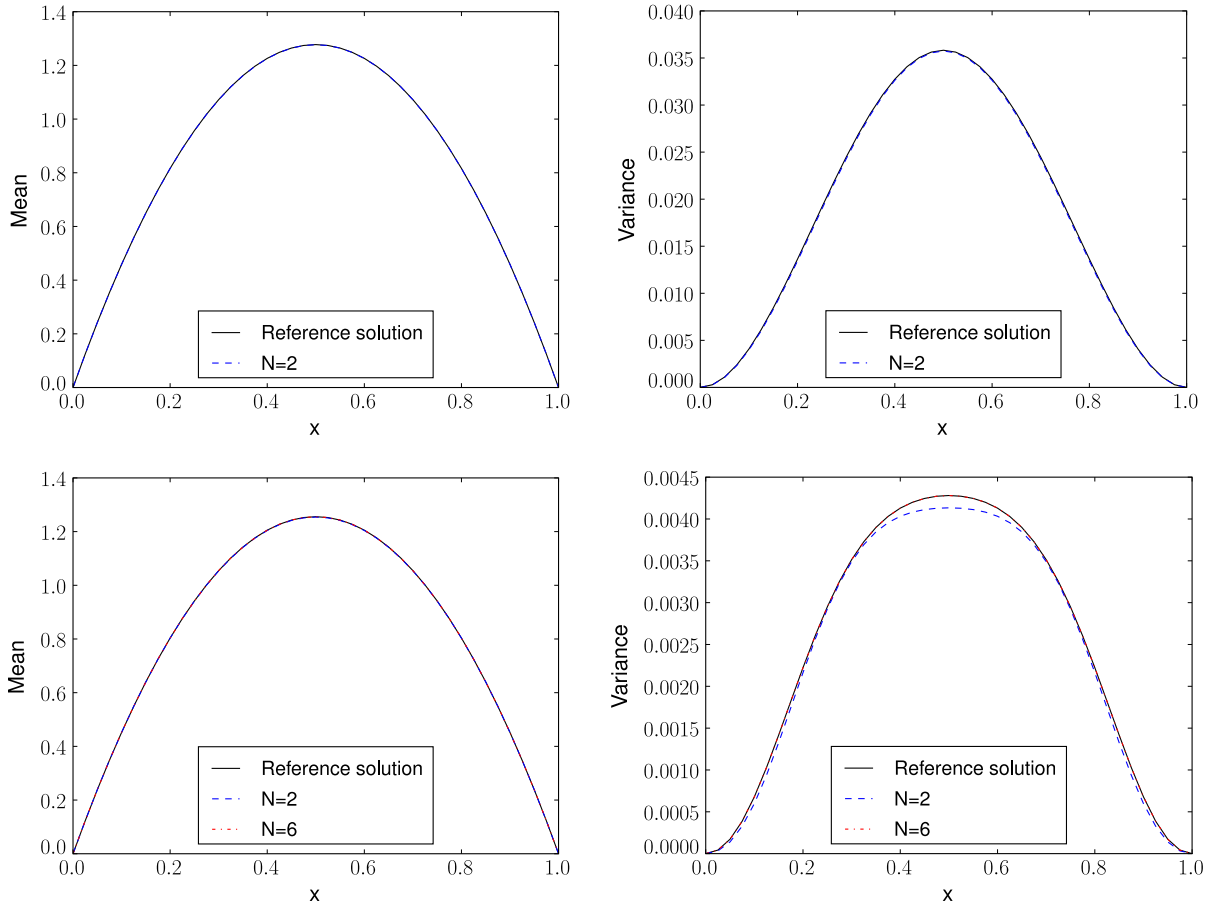


**Fig. 20.** Top: $l_c = 1$, bottom: $l_c = 1/5$. Mean (left) and variance (right) of the solution at $t = 30$ for the nonlinear diffusion equation. DO solutions with $N = 2$ for $l_c = 1$ and with $N = 2, 6$ for $l_c = 1/5$ are plotted and they show good agreement with the exact solution except that the variance with $N = 2$ for $l_c = 1/5$ is different from that of the exact solution.

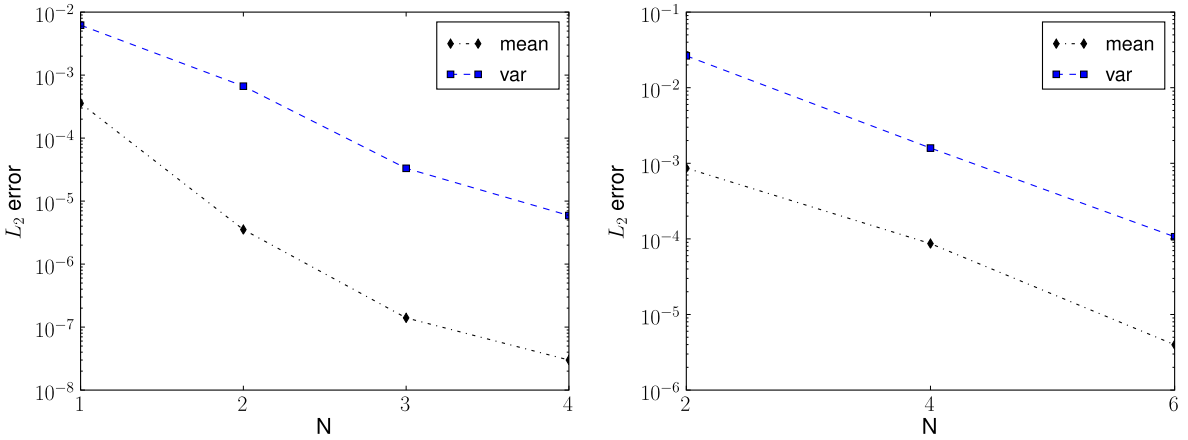


**Fig. 21.** Relative $L_2$ error for the mean and variance at $t = 30$ for $l_c = 1$ (left) and $l_c = 1/5$ (right). Exponential convergence is observed as the number of modes increases.

Burgers equation. Then, we applied the proposed framework with the source of randomness being in the coefficients of the SPDE.

In the advection equation, even when the basis is initiated arbitrarily, the DO evolution equations are capable of following the system satisfactorily in a way that the basis evolves to become the Fourier basis and remains the same thereafter. Clearly, initiating the basis elements as orthogonal polynomials gives larger $L_2$ error compared with the hybrid method but the former example illustrates (i) the effectiveness of the DO method, which tracks the system accurately enough, hence converging to the correct subspace, and (ii) the advantage of using the hybrid approach to initialize problems involving deterministic initial conditions. For the Burgers equation, the hybrid method shows very good agreement with the exact solution with the error being less than $10^{-6}$. This is also the case when the excitation is such that the steady state dynamics involve strongly non-Gaussian statistics with bimodal densities. For the nonlinear diffusion equation, the hybrid method shows very good agreement with the exact solution and converges exponentially with respect to the number of modes.

For both advection and Burgers equation, the $L_2$ error shows that DO is as accurate as PCM. However, DO is more efficient than PCM in terms of computational time, in particular in high-dimensional parametric spaces. In addition, it allows for the expression of higher-order statistics through the probability density function of the stochastic coefficients. This suggests that DO can be a good and cost-effective alternative to PCM.

Further investigations will include a detailed study of adaptive strategies, i.e., adding or removing modes, "on-the-fly" and a multiscale approach to account for some of the energy of high modes that is neglected. Fig. 14 shows the eigenvalues of the solution for the Burgers equation at different times; it is clear that as the system evolves in time, we need more eigenvalues to capture the same percentage of the energy; this can be done adaptively. In addition to this adaptive incorporation of new energetic modes, we can add new "sub-grid-like" terms in the DO representation to account for the action of truncated modes. This is similar to the idea of the multiscale method [28]. Another issue is the reformulation of the DO equations by imposing bi-orthogonality of the basis *and* stochastic coefficients, *i.e.* replacing the DO condition (4) with $\langle u_i(x,t), u_j(x,t)\rangle = \lambda_i \delta_{ij}$ and $E(Y_i Y_j) = \delta_{ij}$ [29]. This leads to a modified system of evolution equations, which, however, is *equivalent* (via a dynamical transformation) to the DO evolution equations. These issues are currently investigated in some more depth and results will be reported in future publication.

## Acknowledgements

We acknowledge financial support from OSD-MURI (Grant No. FA9550-09-1-0613), DOE (Grant No. DE-SC0002542) and NSF (Grant No. DMS-0915077).

## References

[1] T. Sapsis, P. Lermusiaux, Dynamically orthogonal field equations for continuous stochastic dynamical systems, Physica D 238 (2009) 2347–2360.
[2] K. Sobczyk, Stochastic Wave Propagation, Elsevier Publishing Company, 1985.
[3] V. Konotop, L. Vazquez, Nonlinear Random Waves, World Scientific, 1994.
[4] J. Fouque, J. Garnier, G. Papanicolaou, k. Solna, Wave Propagation and Time Reversal in Randomly Layered Media, Springer, 2007.
[5] T. Soong, M. Grigoriu, Random vibration of mechanical and structural systems, PTR Prentice Hall, 1993.
[6] Y. Lin, G. Cai, Probabilistic Structural Dynamics, McGraw-Hill Inc., 1995.
[7] J. Roberts, P. Spanos, Random Vibration and Statistical Linearization, Dover Publications, 2003.
[8] N. Wiener, The homogeneous chaos, American Journal of Mathematics 60 (4) (1938) 897–936.
[9] R. Ghanem, P. Spanos, Stochastic Finite Elements: A Spectral Approach, Springer-Verlag, 1991.

[10] R. Ghanem, J. Red-Horse, Propagation of probabilistic uncertainty in complex physical systems using a stochastic finite element approach, Physica D 133 (1–4) (1999) 137–144.
[11] A. Sarkar, R. Ghanem, Mid-frequency structural dynamics with parameter uncertainty, Computer Methods in Applied Mechanics and Engineering 191 (47–48) (2003) 93–100.
[12] A.J. Chorin, Gaussian fields and random flow, Journal of Fluid Mechanics 63 (01) (1974) 21–32.
[13] O.P.L. Matre, O.M. Knio, H.N. Najm, R.G. Ghanem, A stochastic projection method for fluid flow I. Basic formulation, Journal of Computational Physics 173 (2001) 481–511.
[14] D. Xiu, G.E. Karniadakis, Modeling uncertainty in flow simulations via generalized polynomial chaos, Journal of Computational Physics 187 (2003) 137–167.
[15] O.M. Knio, O.P.L. Matre, Uncertainty propagation in CFD using polynomial chaos decomposition, Fluid Dynamics Research 38 (2006) 616–640.
[16] S. Das, R. Ghanem, S. Finette, Polynomial chaos representation of spatio-temporal random fields from experimental measurements, Journal of Computational Physics 228 (2009) 8726–8751.
[17] D. Xiu, G.E. Karniadakis, The Wiener–Askey polynomial chaos for stochastic differential equations, SIAM Journal on Scientific Computing 24 (2002) 619–644.
[18] D. Xiu, J. Hesthaven, High order collocation methods for differential equations with random inputs, SIAM Journal of Scientific Computing 27 (3) (2005) 1118–1139.
[19] I. Babuska, F. Nobile, R. Tempone, A sparse grid stochastic collocation method for partial differential equations with random input data, SIAM Journal of Numerical Analysis 46 (2008) 2309–2345.
[20] J. Foo, G.E. Karniadakis, Multi-element probabilistic collocation in high dimensions, Journal of Computational Physics 229 (2009) 1536–1557.
[21] Y. Rozanov, Random Fields and Stochastic Partial Differential Equations, Kluwer Academic Press, 1996.
[22] M. Gerritsma, J.-B. van der Steen, P. Vos, G.E. Karniadakis, Time-dependent generalized polynomial chaos, Journal of Computational Physics 229 (2010) 8333–8363.
[23] J. Foo, X. Wan, G.E. Karniadakis, The multi-element probabilistic collocation method: error analysis and simulation, Journal of Computational Physics 227 (2008) 9572–9595.
[24] M. Jardak, C.-H. Su, G.E. Karniadakis, Spectral polynomial chaos solutions of the stochastic advection equation, Journal of Scientific Computing 17 (2002) 319–338.
[25] R.H. Cameron, W.T. Martin, The orthogonal development of non-linear functionals in series of fourier-hermite functionals, The Annals of Mathematics 48 (2) (1947) 385–392.
[26] J. Jacod, P. Protter, Probability Essentials, Springer-Verlag, 2004.
[27] G.E. Karniadakis, S. Sherwin, Spectral/hp Element Methods for Computational Fluid Dynamics, Oxford University Press, 2005.
[28] T.J.R. Hughes, Multiscale phenomena: Green's functions, the Dirichlet-to-Neumann formulation, subgrid scale models, bubbles and the origins of stabilized methods, Computer Methods in Applied Mechanics and Engineering 127 (1995) 387–401.
[29] M. Cheng, T.Y. Hou, Z. Zhang, A dynamically bi-orthogonal stochastic method for time-dependent stochastic partial differential equations I: Derivation and algorithms, Journal of Computational Physics 242 (2013) 843–868.